Pb, Hf and Nd isotope compositions of the two Réunion volcanoes (Indian Ocean): A tale of two small-scale mantle "blobs"?

Delphine Bosch, Janne Blichert-Toft, Frédéric Moynier, Bruce Nelson, Philippe Telouk, Pierre-Yves Gillot, Francis Albarède

Pb, Hf and Nd isotope compositions of the two Réunion volcanoes (Indian Ocean): A tale of two small-scale mantle "blobs"?

Delphine Bosch [a,*], Janne Blichert-Toft [b], Frédéric Moynier [b], Bruce K. Nelson [c], Philippe Telouk [b], Pierre-Yves Gillot [d], Francis Albarède [b]

[a] *Université de Montpellier II, Géosciences Montpellier, CNRS-UMR-5243, Place E. Bataillon, 34095 Montpellier Cedex 05, France*
[b] *Ecole Normale Supérieure de Lyon, Laboratoire des Sciences de la Terre, CNRS UMR-5570, 46, Allée d'Italie, 69364 Lyon Cedex 07, France*
[c] *Department of Earth and Space Sciences, 351310, University of Washington, Seattle WA 98195, USA*
[d] *Université Paris Sud - Institut de Physique du Globe, Laboratoire de Géochronologie, Bat. 504, 91405 Orsay, France*

Abstract

Pb, Hf, Nd and Sr isotopes of basaltic lavas from the two Réunion Island volcanoes are reported in order to examine the origin of the sources feeding these volcanoes and to detect possible changes through time. Samples, chosen to cover the whole lifetime of the two volcanoes (from 2 Ma to present), yield a chemically restricted (compared to OIB lavas) but complex distribution. Réunion plume isotopic characteristics have been defined on the basis of the composition of uncontaminated shield-building lavas from the Piton de la Fournaise volcano. The average ε_{Nd}, ε_{Hf}, $^{87}Sr/^{86}Sr$ and $^{206}Pb/^{204}Pb$, $^{207}Pb/^{204}Pb$, and $^{208}Pb/^{204}Pb$ isotope ratios calculated for this component are +4.4, +9.1, 0.70411, 18.97, 15.59 and 39.03, respectively. In Pb–Pb isotope space, each volcano defines a distinct linear trend but slight variations are also detected within the various volcanic sequences. The Piton des Neiges volcano yields a distinct and significantly more scattered isotopic distribution than Piton de la Fournaise for both Pb, Hf and Nd isotope tracers. A principal component analysis of the Pb isotope data from Piton de la Fournaise reveals a major contribution of the C and EM-1 components (with a clear Dupal flavor) as main components for the modern Réunion plume. The same components have been identified for Piton des Neiges but with a stronger participation of a depleted mantle component and a weaker EM-1 contribution. The compositional change of the lavas erupted by the Piton des Neiges and Piton de la Fournaise volcanoes is attributed to the impingement of two small-scale blobs of plume material at the base of the Réunion lithosphere. Compared to other hot-spots worldwide, in particular Hawaii and Kerguelen, magmas beneath Réunion are generated from a considerably more homogeneous, compositionally more primitive plume higher in ^{206}Pb. Although shallow-level contamination processes have been locally detected they did not alter significantly the composition of the plume magmas. This is tentatively attributed to mantle dynamics producing small, high-velocity blobs that ascend rapidly through the lithosphere, and to the lack of a well-developed magma chamber at depth in the lithosphere.

Keywords: Réunion island; plume; Pb, Hf, Nd isotopes; blob; Piton de la Fournaise: Piton des Neiges; Indian ocean; C component; EM-1 component

1. Introduction

Studies of geochemical and isotopic variations through time of plume lavas erupted from a single volcano or from neighbouring volcanoes are expected to shed light on the composition and evolution of mantle regions involved in a hot-spot environment and to document the processes taking place during magma ascent.

Réunion Island is one of the best known hot-spot volcanoes and has often been compared to the Hawaiian and Kerguelen archipelagos (e.g., Blichert-Toft and Albarède, 1999; Eiler et al., 1996; Eisele et al., 2002; Hofmann and Jochum, 1996; Ingle et al., 2003; Lassiter et al., 1996; Neal et al., 2002). This island is considered as one of the best places worldwide to document the petrological history of relatively simple volcanoes during the different cycles of volcanic eruptions (e.g. Fisk et al., 1988; Graham et al., 1990; McDougall and Compston, 1965). A detailed comparison of the geochemistry between the two volcanoes of the island, Piton des Neiges (PDN) and Piton de la Fournaise (PDF) (Fig. 1), however, is not available. Published Sr, Nd, Pb and He isotopic data from the Réunion volcanoes define a narrow range of variation (Albarède et al., 1997; Albarède and Tamagnan, 1988; Deniel, 1990; Fisk et al., 1988; Graham et al., 1990; Luais, 2004; Oversby, 1972; Staudacher et al., 1990). Recently, subtle patterns of isotopic variability within this range have been identified in Nd and Pb isotope studies from Piton de la Fournaise (Hanyu et al., 2001; Luais, 2004; Vlastelic et al., 2005).

In this study we report Pb, Hf, Nd and Sr isotope analyses of a large sample set of lavas from Réunion Island. This constitutes the first extensive isotopic study of lavas from the two volcanoes at the scale of the island, and in particular the first report of Hf isotope data. In order to detect changes of the isotopic composition through time between the two volcanoes but also between the different sequences of each volcano (i.e., from 2 Ma to present) samples were selected to cover most of the sub-aerial history of the volcanoes. The new data document the spatial and temporal evolution of Réunion plume geochemistry and allow for a comparison with other hot-spot environments.

2. Geological setting

Réunion Island lies 750 km east of Madagascar and is considered to be related to the hot-spot track that trends

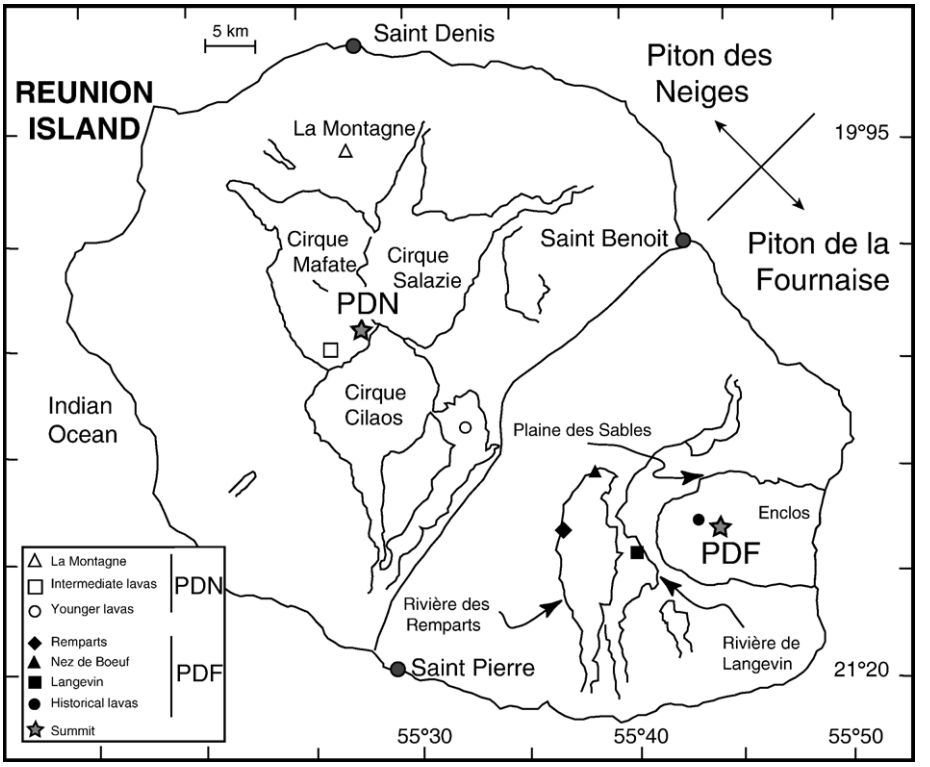

Fig. 1. Map of Réunion island. The island is composed of two large volcanic edifices, Piton des Neiges (PDN), now extinct and located in the northwest, and Piton de la Fournaise (PDF), currently active and situated in the southeast.

Table 1
Pb, Sr, Nd and Hf isotope ratios for lavas from Piton des Neiges and Piton de la Fournaise volcanoes

Samples	Elevation (m)	$^{206}Pb/^{204}Pb$	$^{207}Pb/^{204}Pb$	$^{208}Pb/^{204}Pb$	$^{87}Sr/^{86}Sr$	εSr	$^{143}Nd/^{144}Nd$	εNd	$^{176}Hf/^{177}Hf$	εHf
	Piton de la Fournaise (PDF)									
Les Remparts										
RP01	1690	18.999	15.598	39.070	0.70418 #	−4.6	–	–	–	–
RP02	1670	18.981	15.605	39.052	0.70412 #	−5.4	–	–	–	–
RP03	1630	18.934	15.594	38.989	0.70414 #	−5.2	–	–	–	–
RP04	1605	18.945	15.592	39.001	0.70408 #	−5.9	–	–	–	–
RP05	1590	18.965	15.591	39.021	0.70415 #	−5.0	–	–	–	–
RP06	1550	18.983	15.593	39.039	0.70415 #	−5.0	–	–	–	–
RP07	1540	18.956	15.588	39.017	0.70409 #	−5.8	–	–	–	–
RP09	1390	18.940	15.588	39.013	0.70414 #	−5.1	–	–	–	–
RP10	1370	18.947	15.594	39.012	0.70412 #	−5.4	–	–	–	–
RP11	1345	18.934	15.586	39.001	0.70411 #	−5.5	–	–	–	–
RP12	1330	18.996	15.592	39.059	0.70405 #	−6.3	–	–	–	–
RP13	1280	18.992	15.596	39.073	0.70414 #	−5.0	–	–	–	–
RP14	1270	18.986	15.591	39.056	0.704061±20	−6.2	0.512867±5	4.5	0.283030±5	9.1
							0.512870±6 §	*4.5*	–	–
RP15	1240	19.000	15.596	39.075	0.70408 #	−5.9	–	–	–	–
RP16	1200	18.940	15.591	39.002	0.70415 #	−5.0	–	–	–	–
RP17	1190	18.969	15.593	39.040	0.70406 #	−6.3	–	–	–	–
RP18	1170	18.977	15.583	39.040	0.70416 #	−4.9	–	–	–	–
RP19	1145	18.996	15.596	39.064	0.70405 #	−6.4	–	–	–	–
RP20	1110	18.971	15.599	39.046	0.70410 #	−5.6	–	–	–	–
RP21	1080	18.966	15.590	39.034	0.70411 #	−5.5	–	–	–	–
RP23	990	18.964	15.592	39.029	0.704063±14	−6.2	0.512861±6	4.3	0.283026±6	9.0
							0.512844±7	*4.0*		
RP24	910	18.962	15.583	39.015	0.70405 #	−6.4	–	–	–	–
		18.970	*15.587*	*39.028*						
RP25	890	18.932	15.584	38.981	0.70403 #	−6.6	–	–	–	–
RP26	850	18.941	15.593	39.023	0.70409 #	−5.8	–	–	–	–
RP27	810	18.962	15.592	39.035	0.70407 #	−6.0	–	–	–	–
RP28	790	18.926	15.592	39.002	0.70409 #	−5.9	–	–	–	–
RP29	760	18.924	15.589	38.994	0.70413 #	−5.3	–	–	–	–
RP30	750	18.928	15.591	39.005	0.70412 #	−5.3	–	–	–	–
RP31	740	18.892	15.586	38.955	0.70412 #	−5.4	0.512837±9	3.9	0.283020±7	8.8
RP32	720	18.952	15.593	39.018	0.70406 #	−6.2	0.512861±6	4.3	0.283036±5	9.3
							0.512843±6	*4.0*		
Nez de Bœuf										
R01	1850	18.847	15.607	38.914	–	–	–	–	–	–
R02	1845	18.852	15.582	38.926	–	–	–	–	–	–
R03	1750	18.855	15.592	38.935	–	–	–	–	–	–
R04	1730	18.909	15.592	38.970	–	–	0.512854±6	4.2	0.283011±4	8.4
							0.512844±5	*4.0*		
R05	1720	18.993	15.597	39.041	–	–	–	–	–	–
R06	1710	18.844	15.574	38.883	–	–	0.512851±5	4.1	0.283026±	9.0
R07	1800	18.954	15.594	39.026	–	–	–	–	–	–
R08	1705	18.917	15.588	38.977	–	–	–	–	–	–
R09	1695	18.918	15.592	38.982	–	–	–	–	–	–
R10	1690	18.907	15.588	38.973	–	–	–	–	–	–
R11	1675	18.865	15.603	38.946	0.704222±7	−3.9	0.512840±6	3.9	0.283014±6	8.6
							0.512823±6	*3.6*	*0.283015±6*	*8.6*
R12	1670	19.012	15.604	39.073	0.704056±7	−6.3	0.512843±6	4.0	0.283029±5	9.1
							0.512836±3	*3.9*		
R13	1665	18.912	15.595	38.989	–	–	–	–	–	–

Table 1 (*continued*)

Samples	Elevation (m)	$^{206}Pb/^{204}Pb$	$^{207}Pb/^{204}Pb$	$^{208}Pb/^{204}Pb$	$^{87}Sr/^{86}Sr$	εSr	$^{143}Nd/^{144}Nd$	εNd	$^{176}Hf/^{177}Hf$	εHf
	Piton de la Fournaise (PDF)									
Langevin										
LGV01	2300	18.894	15.587	38.947	0.70412 #	–	–	–	–	–
LGV02	2280	18.895	15.588	38.976	0.70416 #	–	–	–	–	–
LGV03	2260	18.951	15.596	39.028	0.70414 #	–	–	–	–	–
LGV04	2240	18.878	15.581	38.930	0.70410 #	–	–	–	–	–
LGV06	2200	18.888	15.588	38.955	0.70410 #	–	–	–	–	–
LGV07	2190	18.913	15.588	38.962	0.70410 #	–	–	–	–	–
LGV09	2160	18.904	15.591	38.966	0.70406 #	–	–	–	–	–
LGV12	2100	18.911	15.591	38.969	0.70409 #	–	–	–	–	–
LGV13	2080	18.887	15.579	38.933	0.70409 #	–	–	–	–	–
LGV14	2060	18.761	15.535	38.744	0.704212 ± 7	−4.1	0.512826 ± 8	4.0	0.283016 ± 8	8.6
					0.70421 #		*0.512803 ± 19*	*3.2*	*0.283035 ± 7*	*9.3*
							0.512811 ± 6	*3.4*	*0.283017 ± 14*	*8.7*
LGV15	2040	18.846	15.582	38.915	0.70406 #	–	–	–	–	–
LGV16	1990	18.894	15.587	38.953	0.70421 #	–	–	–	–	–
LGV17	1980	18.888	15.589	38.956	0.70421 #	−3.9	0.512839 ± 7	3.9	0.283019 ± 11	8.7
							0.512795 ± 13	*3.1*	*0.283028 ± 5*	*9.0*
							0.512822 ± 6	*3.6*		
LGV18	1985	18.905	15.594	38.978	0.70423 #	–	–	–	–	–
LGV20	1960	18.920	15.585	38.976	0.70413 #	–	–	–	–	–
LGV21	1930	18.961	15.598	39.024	0.70412#	–	–	–	–	–
LGV22	1910	18.968	15.596	39.016	0.70410 #	−5.6	0.512858 ± 5	4.3	0.283039 ± 7	9.4
							0.512852 ± 5	*4.2*		
LGV23	1905	18.851	15.583	38.914	0.70416 #	–	–	–	–	–
LGV25	1870	18.881	15.588	38.946	0.70417 #	–	–	–	–	–
LGV26	1850	18.858	15.592	38.928	0.70404 #	–	–	–	–	–
		18.857	*15.587*	*38.921*	–	–	–	–	–	–
LGV27	1830	18.874	15.584	38.928	0.70405 #	–	–	–	–	–
LGV28	1820	18.838	15.590	38.908	0.70409 #	−5.8	0.512858 ± 6	4.3	0.283036 ± 4	9.3
							0.512844 ± 6	*4.0*		
LGV29	1815	18.853	15.588	38.916	0.70411 #	–	–	–	–	–
Historical samples										
	Year of eruption (y)									
R1301	1700	18.915	15.590	39.001		–	–	–	–	–
O2201	1802	18.876	15.578	38.937	–	–	–	–	–	–
R1201	1905	18.915	15.590	39.002	–	–	–	–	–	–
Q1301	1915	18.951	15.596	39.010	–	–	–	–	–	–
S1401	1927	18.861	15.584	38.933	–	–	–	–	–	–
Q1401		18.938	15.593	39.004	–	–	–	–	–	–
T1902	1927	18.868	15.575	38.866	0.704159 ± 14	−4.8	0.512841 ± 4	4.0	0.283027 ± 13	9.0
							0.512827 ± 20	*3.7*	*0.283057 ± 6*	*10.1*
T2101	1927	18.885	15.587	38.968	–	–	–	–	–	–
T1602	1931	18.790	15.564	38.824	0.704117 ± 14	−5.4	0.512852 ± 5	4.2	0.283025 ± 11	9.0
							0.512835 ± 3	*3.8*	*0.283040 ± 5*	*9.5*
L2001	1934	18.931	15.592	38.993	0.704118 ± 11	−5.4	0.512848 ± 5	4.1	0.283030 ± 4	9.1
							0.512831 ± 3	*3.8*		
P1601	1939	18.890	15.586	38.960	–	–	–	–	–	–
N2201	1943	18.898	15.589	38.971	–	–	–	–	–	–
O2202	1943	18.870	15.588	38.934	–	–	–	–	–	–
M1701	1945	18.813	15.589	38.870	0.704156 ± 17	−4.9	0.512858 ± 4	4.3	0.283031 ± 4	9.2
							0.512851 ± 6 §	*4.2*		
R1801		18.919	15.586	38.970	–	–	–	–	–	–

(continued on next page)

Table 1 (*continued*)

Historical samples	Elevation (m)	$^{206}Pb/^{204}Pb$	$^{207}Pb/^{204}Pb$	$^{208}Pb/^{204}Pb$	$^{87}Sr/^{86}Sr$	εSr	$^{143}Nd/^{144}Nd$	εNd	$^{176}Hf/^{177}Hf$	εHf
	Year of eruption (y)									
R2301		18.888	15.586	38.956	–	–	–	–	–	–
R1602		18.900	15.590	38.965		–	–	–	–	–
Q1303		18.851	15.581	38.916	–	–	–	–	–	–
T1904	1953	18.880	15.583	38.947	–	–	–	–	–	–
S2301		18.877	15.582	38.932	–	–	–	–	–	–
S1201	b 1949	18.909	15.584	38.985	0.704185 ± 14	−4.5	0.512851 ± 5	4.1	0.283033 ± 5	9.2
							0.512834 ± 3	*3.8*		
	Piton des Neiges (PDN)									
	Age (kyr)									
Oldest lavas										
00RU8G	2000/2150	19.045	15.579	38.894	–	–	0.512813 ± 15 §	3.4	0.28303 ± 6	9.1
00RU7G	2000/2150	18.975	15.541	38.805	–	–	0.512805 ± 11 §	3.3	0.283016 ± 6	8.6
00RU15	2000/2150	19.011	15.554	38.848	–	–	0.512813 ± 11 §	3.4	0.283033 ± 7	9.2
00RU13	2000/2150	19.067	15.582	38.938	–	–	0.512839 ± 12 §	3.9	0.283026 ± 9	9.0
00RU9G	2000/2150	18.938	15.551	38.796	–	–	0.512840 ± 10 §	3.9	0.283047 ± 5	9.7
							0.512824 ± 3	*3.6*		
00RU26	2000/2150	19.075	15.589	38.962	–	–	0.512815 ± 10 §	3.5	0.283019 ± 8	8.7
							0.512812 ± 4	*3.4*		
00RU08	2000/2150	18.918	15.566	38.757	–	–	0.512806 ± 10	3.3	0.283014 ± 8	8.6
							0.512798 ± 10 §	*3.1*		
Intermediate samples										
PN67G1	1400	19.002	15.564	38.869	–	–	0.512828 ± 11 §	3.7	0.283051 ± 13	9.9
PN69H4	1200	18.969	15.569	38.813	–	–	0.512841 ± 8 §	4.0	0.283033 ± 6	9.2
PN67P1	1040	18.973	15.581	38.858	–	–	0.512841 ± 14	4.0	0.283024 ± 7	8.9
PN60K	946	18.943	15.568	38.827	–	–	0.512809 ± 6	3.3	0.283046 ± 9	9.7
PN69H18	680	18.992	15.572	38.852	–	–	0.512822 ± 7 §	3.6	0.283014 ± 8	8.6
							0.512833 ± 6	*3.8*		
Younger lavas										
PN69T1	577	18.723	15.551	38.630	–	–	0.512834 ± 7 §	3.8	0.283067 ± 8	10.4
PN60D	452	18.921	15.5571	38.722	–	–	0.512851 ± 7 §	4.1	0.283082 ± 9	11.0
PN60A	374	18.762	15.560	38.700	–	–	0.512797 ± 12 §	3.1	0.283039 ± 7	9.4

Uncertainties reported on Sr, Nd and Hf measured isotope ratios are $2\sigma/n^{1/2}$ analytical errors in last decimal place, where n is the number of measured isotopic ratios. Analytical errors on Pb isotope ratios are better than 300 ppm. The $^{87}Sr/^{86}Sr$ isotope ratios labelled # are from Albarède et al. (1997). The $^{143}Nd/^{144}Nd$ ratios labelled § were analysed by MC-ICP-MS. ε_{Sr}, ε_{Nd} and ε_{Hf} were calculated using $(^{87}Sr/^{86}Sr)_{CHUR(0)} = 0.7045$, $(^{143}Nd/^{144}Nd)_{CHUR(0)} = 0.512638$ and $(^{176}Hf/^{177}Hf)_{CHUR(0)} = 0.282772$, respectively. Italic ratios are duplicates. –: not analysed.

northeast through Mauritius Island, along the Mascarene Plateau and ends in the Deccan Traps of western India (e.g., Duncan et al., 1989; Morgan, 1981). Burke (1996) challenged this model and proposed that Réunion Island results from the activity of a younger hot-spot unrelated to the track of the Deccan hot-spot. In 1997, Albarède et al. (1997) proposed that each volcano results from impingement at the base of the lithosphere of a blob representing a solitary wave of hot-spot material with a radius of approximately 100 km.

The island consists of two volcanoes, 30 km apart, that were active simultaneously over at least 500 000 years, from ca. 530 to 30 ka (Gillot et al., 1990). They show strong petrological similarities with a predominance of basalts and hawaiites (Albarède and Tamagnan, 1988; Fisk et al., 1988; Ludden, 1978; Nativel et al., 1979; Sobolev and Nikogosian, 1994).

Piton des Neiges is the oldest volcano of the island with the earliest eruptive cycle dated at ca. 2 Ma and the youngest at around 30 ka (Gillot et al., 1990; McDougall, 1971; Rocher, 1990). This volcano is now extinct and occupies the northwestern two thirds of the island. The oldest series (previously called the Oceanite Series) belongs to the area known as La Montagne (McDougall, 1971) and consists of transitional to silica-saturated alkaline lavas. This series, which erupted during the

shield-building volcanic phase between 2.1 Ma and *c.* 440 ka, can be divided into three major groups: a first group mainly comprised of olivine basalts with ages between 2.1 and 1.9 Ma, an intermediate phase with eruption of basalts, and a last younger phase corresponding to the end of shield-building activity between 580 and 440 ka (Deniel, 1990). The late-stage capping lavas, corresponding to the construction of a strato-volcano within the eroded shield volcano, are made of ignimbrites and alkaline under-saturated lavas with ages of 180 to 68 ka (Gillot et al., 1990; Rocher, 1990). The younger Piton des Neiges basalts are silica over-saturated alkaline lavas and are contemporaneous with the oldest lavas of Piton de la Fournaise (from 570 to 300 ka) (Rançon et al., 1989). Fifteen lavas from Piton des Neiges, selected to cover most of its lifetime (from 2150 to 374 ka), were selected for this study.

The large Piton de la Fournaise volcano erupted successive series of lavas that evolved from mildly alkalic very early on to tholeiitic for most of its volcanic history (Albarède et al., 1997). On the basis of K−Ar data (Gillot et al., 1990), three distinct prehistoric eruptive cycles have been recognized and dated at 527−290 ka (Rivière des Remparts, RP), 180−105 ka (Nez de Boeuf, NB) and 70−40 ka (Langevin, LGV). We also studied modern lava flows erupted between 1700 and 1956 (Fig. 1). Picrites, basalts, plagioclase-rich basalts and differentiated samples have been identified within the four sequences. The oldest series (RP) consists of basalts, picrites, differentiated lavas and plagioclase-cumulates with scarce gabbroic fragments (Bachélery and Mairine, 1990). A drill hole in the Grand Brulé (Enclos Fouqué) encountered gabbros, wehrlites and dunites with traces of hydrothermal alteration (Augé et al., 1989; Lerebour et al., 1989). The hiatus between the RP series and the three other sequences (no samples dated between 290 ka and 219 ka) coincides with a major discontinuity between the older series and the most recent shield, possibly reflecting low volcanic activity, intense erosion or formation of a new caldera (Gillot et al., 1990). The NB series consists of olivine-bearing basalts and is thought to represent the volcanic infilling of an ancient canyon. This sequence is made of lavas erupted after the major discontinuity observed between the RP series (520−290 ka) and the more recent shield (built at approximately 150−130 ka). The NB series incorporates the occurrence of major extended discontinuities between the various lava flows (Bachélery and Mairine, 1990). The LGV sequence is made up of basalts and picrites with few aphyric samples and one ankaramite (LGV14). The historic lavas (M) correspond to samples taken from the east flank of the Dolomieu volcano. They consist of basalts and picrites related to major volcanic pulses disrupting pre-existing olivine-rich cumulates (Albarède and Tamagnan, 1988). Eighty-seven samples that encompass the total range of lavas erupted during the entire lifetime of Piton de la Fournaise have been analysed.

3. Analytical methods

Powdered samples were weighed to obtain approximately 100 to 200 ng of Sr, Nd, Pb and Hf. A leaching step with 6 N HCl during 30 min at 65 °C was done before acid digestion. Samples were dissolved during 36−48 h on a hot plate with a mixture of HF and HNO_3. After evaporation to dryness, 1 ml of HNO_3 was added to the residue and kept at about 90 °C for 12−24 h. For Pb separation, after complete evaporation, 0.5 ml of 8 N HBr was added to the sample and kept at 70 °C for 2−3 h before another complete evaporation. The chemical separation of Pb was done using 50 μl of anion exchange resin (AG1X8, 200−400 mesh) with samples being loaded and washed in 0.5 N HBr. Lead was then eluted in 6 N HCl. Lead blanks were less than 40 pg and are considered negligible for the present analyses. Hafnium chemical purification followed the method outlined by Blichert-Toft et al. (1997). Strontium isotopes were separated using Sr Eichrom resin (Pin et al., 1994). Neodymium isotopes were separated following Richard et al. (1976) including a first step of REE separation (using AG50WX12 cation exchange resin) followed by two steps of Nd purification using the HDEHP technique. Strontium, Nd and Hf total procedural blanks were less than 50 pg, 15 pg and 20 pg, respectively. Strontium isotope ratios were measured at the University of Toulouse. The other Sr isotopic data, labelled as # in Table 1, are from a previous study (Albarède et al., 1997). Neodymium isotopes were measured either by thermal ionization mass spectrometry at the University of Montpellier II or, for Nd ratios labelled as § in Table 1, by multi-collector inductively-coupled plasma mass spectrometry (MC-ICP-MS; VG Plasma 54) at the Ecole Normale Supérieure in Lyon (ENSL). Details about analytical parameters, including reproducibility, accuracy and standards, are available online in Supplementary data 1 in the Appendix. Lead, Hf and some Nd (samples labelled § in Table 1) isotope compositions were determined by MC-ICP-MS using the VG Plasma 54 at ENSL (White et al., 2000; Blichert-Toft et al., 1997; Luais et al., 1997; Albarède et al., 2004).

4. Results

The Pb, Sr, Hf and Nd isotope data are given in Table 1. $^{206}Pb/^{204}Pb$, $^{208}Pb/^{204}Pb$, $^{143}Nd/^{144}Nd$ and $^{176}Hf/^{177}Hf$ isotope ratios are reported as a function of age (Piton des Neiges) or elevation (Piton de la Fournaise) (Fig. 2a and b).

4.1. Piton des Neiges lavas

Taken as a whole, the fifteen analyzed Piton des Neiges lavas yield a limited yet significant range of Pb isotope ratios with $^{206}Pb/^{204}Pb$ = 18.723−19.075, $^{207}Pb/^{204}Pb$ = 15.541−15.589 and $^{208}Pb/^{204}Pb$ = 38.630−38.962. Omitting two samples (PN69T1, PN60A) with the least radiogenic Pb isotope ratios significantly reduces the scatter observed for $^{206}Pb/^{204}Pb$ (18.918−19.075) and $^{208}Pb/^{204}Pb$ (38.722−38.962). The range remains essentially unchanged for $^{207}Pb/^{204}Pb$. In the $^{208}Pb/^{204}Pb$ vs $^{206}Pb/^{204}Pb$ diagram, the remaining samples define an alignment (*Trend 1* in Fig. 3a) characterized by a slope of 1.51 and a correlation coefficient of 0.91 (n = 13). No obvious relationship exists between Pb isotope ratios and the age of the lavas. The seven oldest lavas encompass the whole range of variation of the Piton des Neiges samples, whereas the younger lavas yield less radiogenic Pb (Fig. 3). With respect to the Northern Hemisphere Reference Line (Hart, 1988), all samples yield high $^{208}Pb/^{204}Pb$ and $^{207}Pb/^{204}Pb$ ratios for a given $^{206}Pb/^{204}Pb$ value, which is typical of OIB and MORB from the Indian Ocean (see Indian Ocean MORB and OIB compilation in GEOROC database [http://georoc.mpch-mainz.gwdg.de/georoc/]). The five samples from the intermediate series display the most homogeneous Pb isotope compositions of all analyzed samples. The ε_{Hf} and ε_{Nd} values of all Piton des Neiges lavas display a significant range of variation from + 8.6 to + 11.0 and + 3.1 to + 4.1, respectively. Lavas from the younger series have the most scattered and the highest ε_{Hf} (from + 9.4 to + 11.0).

4.2. Piton de la Fournaise lavas

The 87 lavas analysed from the Piton de la Fournaise volcano display a limited but complex Pb isotope distribution within the different isotope spaces. As for the Piton des Neiges samples, lavas erupted by Piton de la Fournaise display similarities with Indian Ocean OIBs and MORBs. Hafnium and Nd isotopes define a small domain of variation with ε_{Hf} =+ 8.4 to + 10.1 and ε_{Nd} =+ 3.1 to + 4.5. Most analyses define a restricted field defined by $^{206}Pb/^{204}Pb$ = 18.838−19.012, $^{207}Pb/^{204}Pb$ = 15.574−15.607, and $^{208}Pb/^{204}Pb$ = 38.866−39.075, respectively. In the $^{208}Pb/^{204}Pb$ versus $^{206}Pb/^{204}Pb$ diagram, these samples define a correlation-line (referred to as *Trend 2*) nearly parallel to that defined by the Piton des Neiges samples (slope= 0.98, r^2 = 0.96, n = 80) (Fig. 3a). Most samples from the four Piton de la Fournaise series plot along this line and exhibit a broad correlation between the age of the series and the Pb isotope compositions, with the oldest sequence being characterized by the most radiogenic Pb isotope compositions. A few samples have significantly less radiogenic Pb and define an additional trend (referred to as *Trend 2′* in Fig. 3a), which clearly points toward the ankaramite LGV14 from the Langevin sequence. However, these samples yield ε_{Hf} (+9.0 and + 9.2) and ε_{Nd} (+ 4.2 and + 4.3) values indistinguishable from those of the other Piton de la Fournaise samples. The Trend 2' comprises at least two historical lavas (T1602 and M1701) but also some Langevin and Nez de Boeuf samples and two of the three youngest lavas from Piton des Neiges. The Sr isotope compositions measured for the Piton de la Fournaise lavas vary from 0.704034 to 0.704227 (this study and Albarède et al., 1997; Albarède and Tamagnan, 1988) and are within the range of values reported earlier (Fisk et al., 1988; Luais, 2004; Ludden, 1978). Previous Nd isotope data from Piton de la Fournaise (Luais, 2004) showed a temporal increase of the Nd isotope ratios (Fig. 2b). Although our study is based on fewer measurements such an increase of $^{143}Nd/^{144}Nd$ through time is not observed. Instead, we

Fig. 2. (a) — $^{206}Pb/^{204}Pb$ and $^{208}Pb/^{204}Pb$ versus age (in ka) for the Piton des Neiges volcano and versus elevation (m) for the Piton de la Fournaise volcano. The symbols encompass the error margins. For Piton des Neiges, the age range for the various lava series are the following: La Montagne (2 Ma), Intermediate series (from 2 Ma to 600 ka), Younger lavas (less than 577 ka). For the Piton de la Fournaise lavas, the altitude is broadly correlated with the ages of the lava flows: with increasing height, Les Remparts (527−290 ka), Nez de Bœuf (180−105 ka), Langevin (70−40 ka). K−Ar ages are from (Gillot et al., 1990). For the historical lava flows, the elevation at which the samples were taken are not reported and samples have been arbitrarily positioned up to the Langevin series in the order of dates of eruption. Symbols are the same as those in Fig. 1. (b) ε_{Nd} and ε_{Hf} variations. Neodymium isotope results from previous studies are reported for comparison: grey diamond: Les Remparts (Luais, 2004), grey square: Langevin (Luais, 2004), grey small dot: historical lavas (Luais, 2004), grey triangle: historical lavas (Vlastelic, unpublished data), cross: lavas dredged from the submarine flanks of Réunion Island (Fretzdorff and Haase, 2002). The grey domain encompasses the totality of our Piton de la Fournaise Nd isotope data and includes data from both Vlastelic (unpublished data) and Fretzdorff and Haase (2002).

find a nearly constant Nd isotopic composition. Our Remparts Nd isotope data are ~ 1 ε_{Nd} higher than those reported by Luais (2004), whereas historic samples are ~1 ε_{Nd} lower. The temporal increase of Nd isotopes at nearly constant Sr ratios is a distinctive feature of these data and is not shown by other OIB. Moreover, very

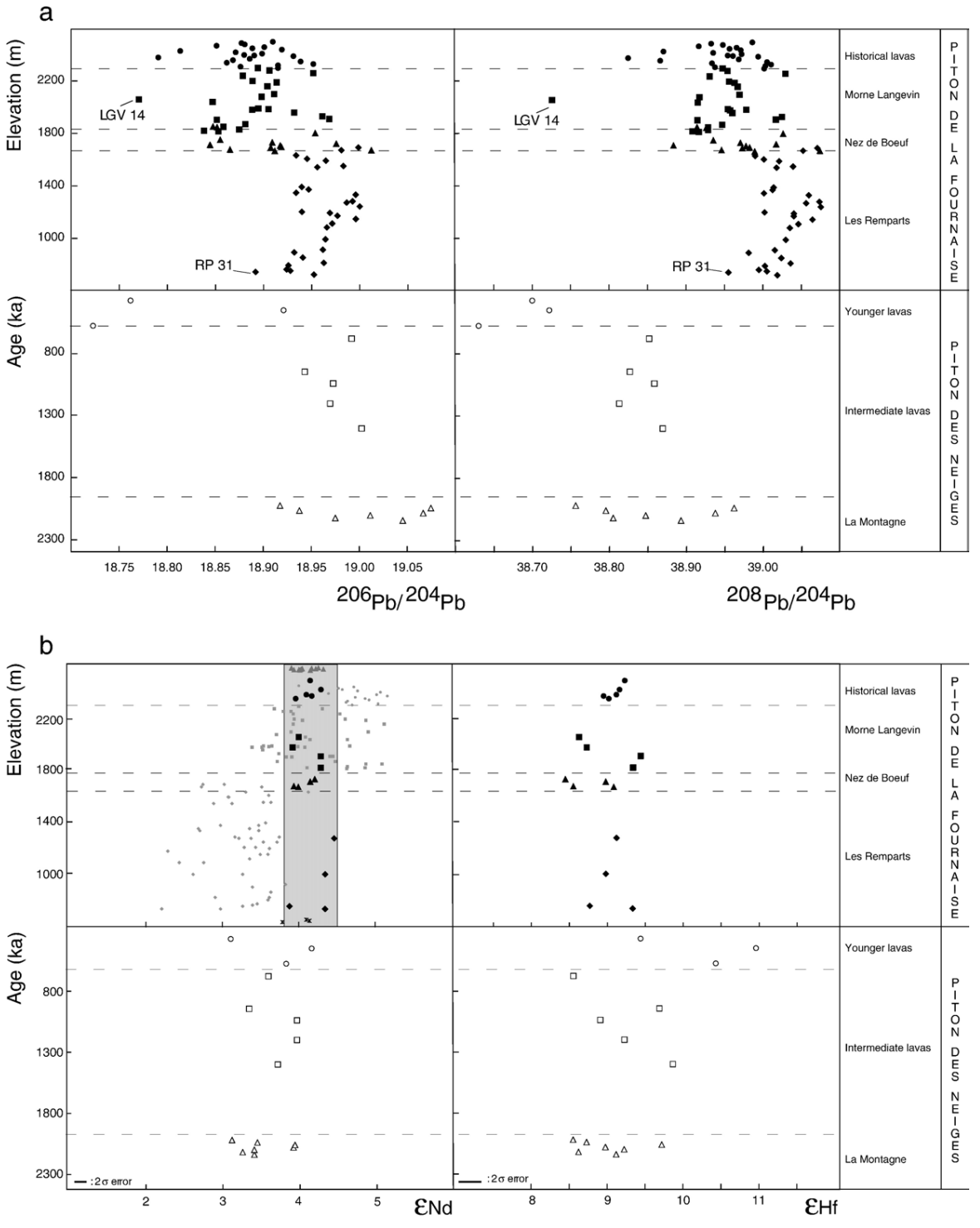

recent samples from Piton de la Fournaise (1998–2006; I. Vlastelic, unpub. data) as well as very old submarine samples (taken from seamounts covered by thick Fe–Mn deposits; Fretzdorff and Haase, 2002) display the same narrow Nd isotope range as our Piton de la Fournaise Nd isotope variation (Fig. 2b). Taken together, these observations do not support a $^{143}Nd/^{144}Nd$ increase through time in Piton de la Fournaise lavas. The trend reported by Luais (2004) may be an analytical artefact from not separating Nd from the other REEs prior to MC-ICP-MS analysis.

In Pb–Pb, Hf–Nd, Hf–$^{206}Pb/^{204}Pb$ and Nd–$^{206}Pb/^{204}Pb$ diagrams (Figs. 3–5), the RP lavas display more restricted and homogeneous compositions in comparison with all other sequences (including the Piton des Neiges samples). One sample containing disaggregated gabbroic fragments (RP31) yields slightly less radiogenic Nd, Hf and Pb isotope compositions compared to other RP samples (Table 1). The ankaramite (LGV14), which is the most magnesian of all of the analyzed PDF lavas (MgO= 26.67 wt.%; Albarède et al., 1997), has the lowest $^{208}Pb/^{204}Pb$ and $^{206}Pb/^{204}Pb$

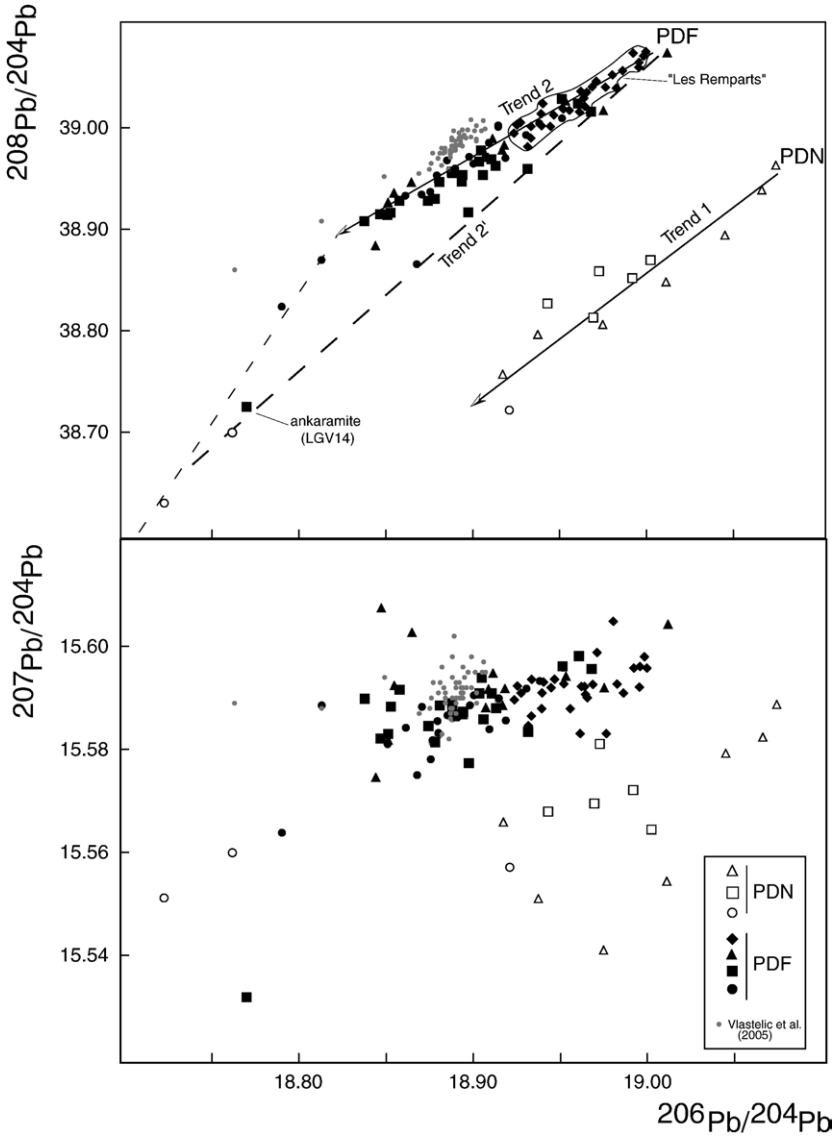

Fig. 3. (a) $^{206}Pb/^{204}Pb$ versus $^{207}Pb/^{204}Pb$ and (b) $^{206}Pb/^{204}Pb$ versus $^{208}Pb/^{204}Pb$ for Piton de la Fournaise and Piton des Neiges lava flows. Trend 1 corresponds to an apparent mixing line for samples from Piton des Neiges. Trend 2 and 2′ are apparent pseudo-binary mixing lines defined by samples from Piton de la Fournaise. See text for discussion.

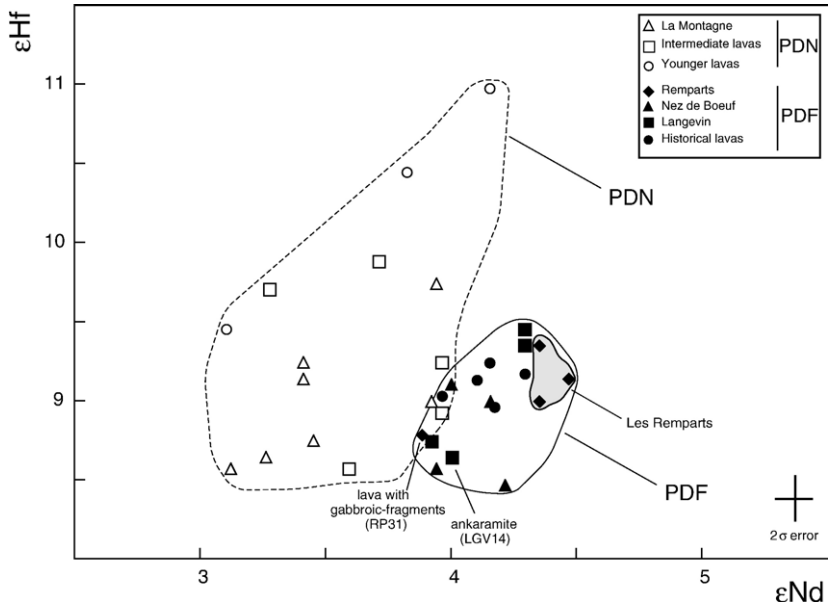

Fig. 4. ε_{Hf} versus ε_{Nd} for Réunion lavas. Piton de la Fournaise lavas display a very restricted field (full line) compared to the Piton des Neiges domain (dashed line). The grey domain is considered as closest to the Réunion plume composition as defined in this study.

isotope compositions and one of the highest $^{87}Sr/^{86}Sr$ ratios of the present data set. Nevertheless, its ε_{Nd} and ε_{Hf} values are not distinct from the rest of the PDF lavas (Table 1). LGV14 has high CaO/Al_2O_3 and Sc/Yb ratios combined with very low FeO/MgO (Albarède et al., 1997). In Fig. 3a, it is located at the lower extremity of Trend 2′. Two historical samples (T1602, M1701) display significantly lower $^{206}Pb/^{204}Pb$ and $^{208}Pb/^{204}Pb$ values than samples from other PDF sequences (Fig. 3a). These two samples partly overlap the 1998–2002 historical samples analysed by Vlastelic et al. (2005) (Fig. 3a).

5. Discussion

5.1. Identification of various mantle components in the Réunion plume

Plume models suggest that plumes are compositionally composite (Campbell and Griffiths, 1990; Farnetani et al., 1996). If plume sources contain a variety of recycled material (igneous and sedimentary sections of the oceanic crust, oceanic lithospheric mantle, plume heads, etc…) and, in addition, if this material is recycled at different times during Earth's history, plume material is not expected to be isotopically homogeneous.

The RP lavas may represent a dominant plume component at Piton de la Fournaise. The RP lavas span a long time interval (520–290 ka) and are conspicuously homogeneous. As shown in studies of other hot-spots, the contribution of a plume component is often positively correlated with lava production rates (Hanan and Schilling, 1997; Schilling, 1991). The RP volcanic sequence erupted during the shield-building stage of Piton de la Fournaise activity and corresponds to high volcanic production rates (more than 1000 m of lavas now exposed at the surface). It may therefore be regarded as little contaminated at shallow level and as representing an unmodified plume composition. Representative isotopic values for this component are $\varepsilon_{Nd} = +4.4$, $\varepsilon_{Hf} = +9.1$, $^{87}Sr/^{86}Sr = 0.70411$, $^{206}Pb/^{204}Pb = 18.97$, $^{207}Pb/^{204}Pb = 15.59$, and $^{208}Pb/^{204}Pb = 39.03$.

It remains to be determined whether the isotopic variability of Réunion lavas reflects a heterogeneous source, as in Hawaii and Iceland (e.g. Hofmann, 1997), or whether shallow level entrainment of upper mantle and contamination by lithosphere has modified an originally homogeneous isotopic signal (Eiler et al., 1996; Hauri et al., 1994). Participation of a small amount of MORB-type mantle has been proposed for the composition of the plume magmas supplying recent shield lavas in Mauritius (Peng and Mahoney, 1995; Paul et al., 2005; Nohda et al., 2005). Entrainment of the ambient mantle as envisioned by Hauri et al. (1994) is dynamically improbable because temperature-dependent viscosity efficiently decouples the plume conduit from the surrounding mantle (Farnetani and Richards, 1994; Olson, 1993). Shallow contamination of

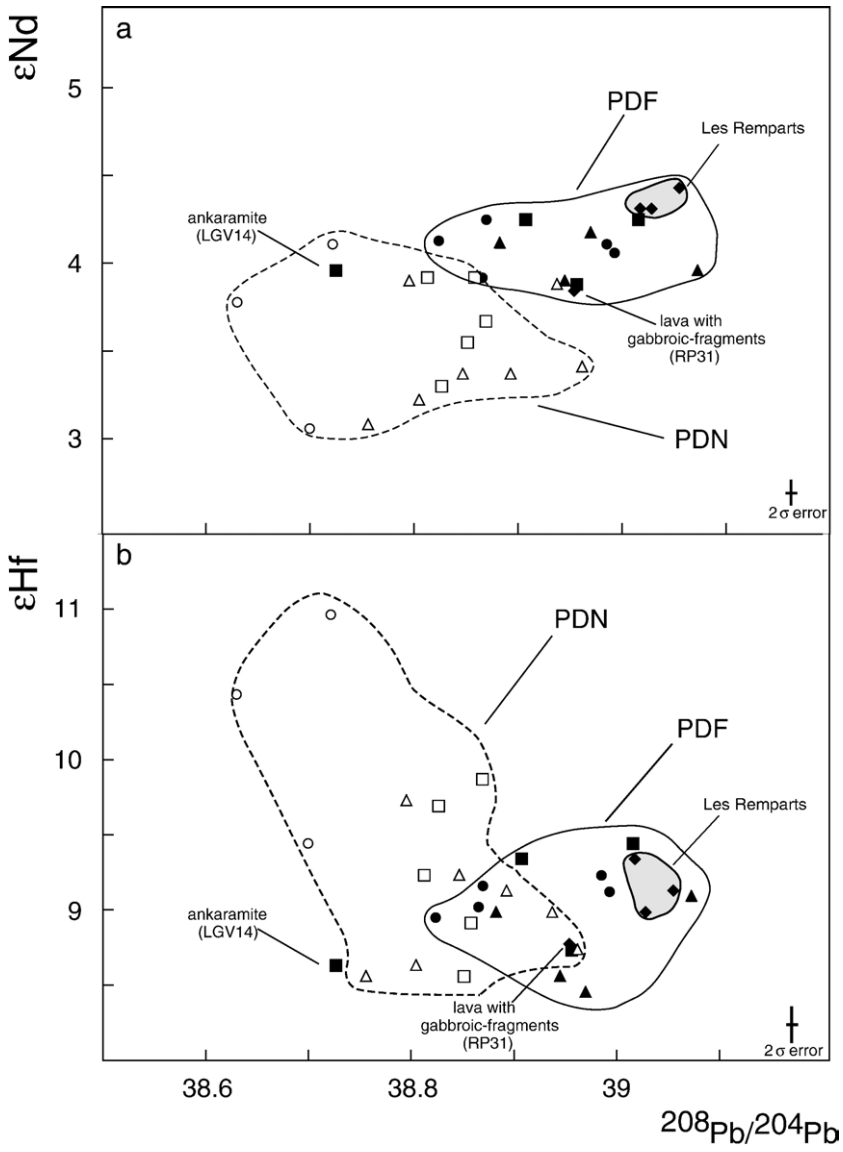

Fig. 5. (a) $^{206}Pb/^{204}Pb$ versus ε_{Hf} and (b) $^{206}Pb/^{204}Pb$ versus ε_{Nd} for Piton des Neiges and Piton de la Fournaise lavas. Symbols as in Fig. 4.

upwelling hot-spot material ponding beneath the lithosphere by the upper mantle and the oceanic crust would be more likely. In the case of Hawaii, however, Blichert-Toft et al. (1999) observed a strongly curved mixing array between ε_{Hf} and $^{206}Pb/^{204}Pb$, that clearly leaves asthenospheric and lithospheric material off the trend. Huang and Frey (2003) pointed out that more than two components are necessary to account for the isotope geochemistry of Hawaiian lavas, but this additional complexity does not alter the simple geometrical relationship that excludes the depleted mantle from the mixing array. For the Réunion volcanoes, unfortunately, the range of isotopic variation is insufficient to obtain a well-defined mixing array.

We first consider the possibility that the Nd, Hf, and Pb isotope variability of the modern Réunion plume results from minor addition of depleted mantle to the pure plume-source material. Such depleted MORB-source mantle would have a composition close to that of the basalts from site 706-701 of ODP Leg 115 (White et al., 1990), which have isotopic characteristics similar to those of typical Indian Ocean basalts (Xu and Castillo, 2004; Zhang et al., 2005). The contribution of this depleted component, however, must be limited compared to Hawaii and some

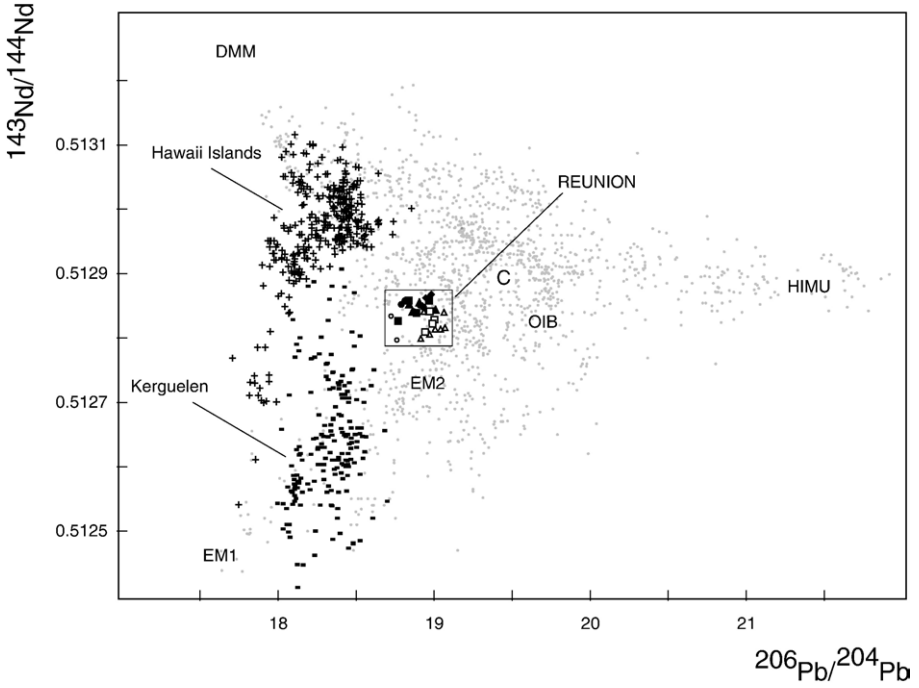

Fig. 6. $^{206}Pb/^{204}Pb$ versus $^{143}Nd/^{144}Nd$ for Réunion lavas. The OIB, Hawaii islands and Kerguelen fields are from the GEOROC database [http://georoca.mpch-mainz.gwdg.de/georoc/]. DMM, HIMU, EM-1, EM-2 and C are from Zindler and Hart (1986), Salters and White (1998) and Hanan et al. (2000). Symbols as in Fig. 4.

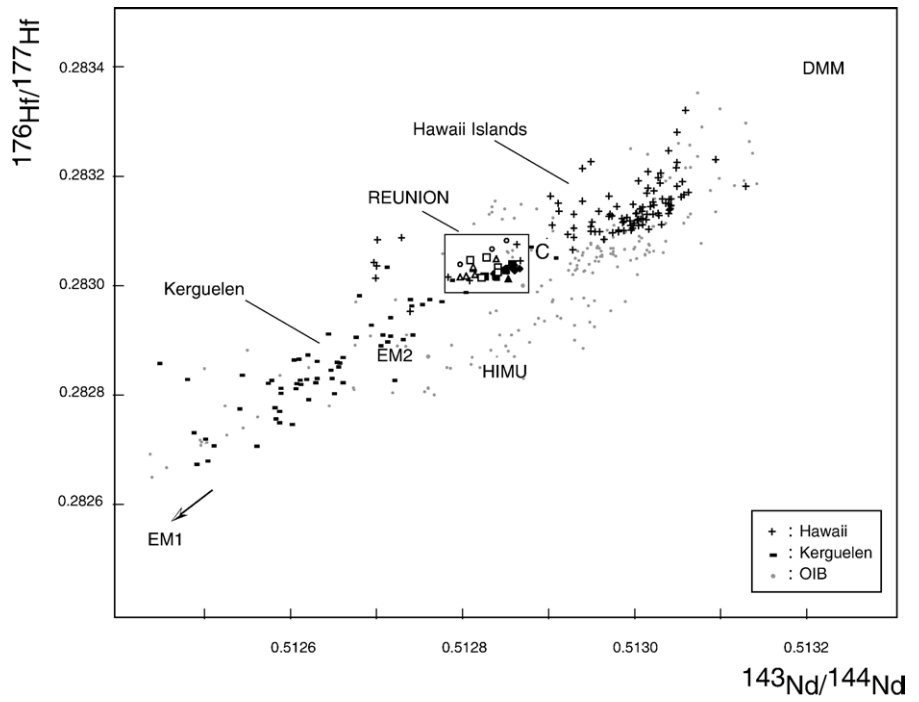

Fig. 7. $^{143}Nd/^{144}Nd$ versus $^{176}Hf/^{177}Hf$ for Réunion Island lavas. The OIB, Hawaii islands and Kerguelen fields are from the GEOROC database [http://georoca.mpch-mainz.gwdg.de/georoc/]. DMM, HIMU, EM-1, EM-2 and C are from Zindler and Hart (1986), Salters and White (1998)and Hanan et al. (2000). Symbols as in Fig. 4.

other areas of the western Indian Ocean (White et al., 1990). For example, in the $^{143}Nd/^{144}Nd$ versus $^{206}Pb/^{204}Pb$ plot (Fig. 6), Réunion plots much farther from the depleted mantle component than does Hawaii (also for Nd–Hf, Pb–Pb and Hf–$^{206}Pb/^{204}Pb$ plots; Figs. 7, 8 and Supplementary data 3 in the Appendix).

An alternative interpretation is heterogeneity within the plume itself. In this case, Trend 2 of Piton de la Fournaise in Pb isotope space requires at least two components, while one additional component is needed to account for Trend 2' toward the ankaramite and the other samples plotting below the main trend. A principal

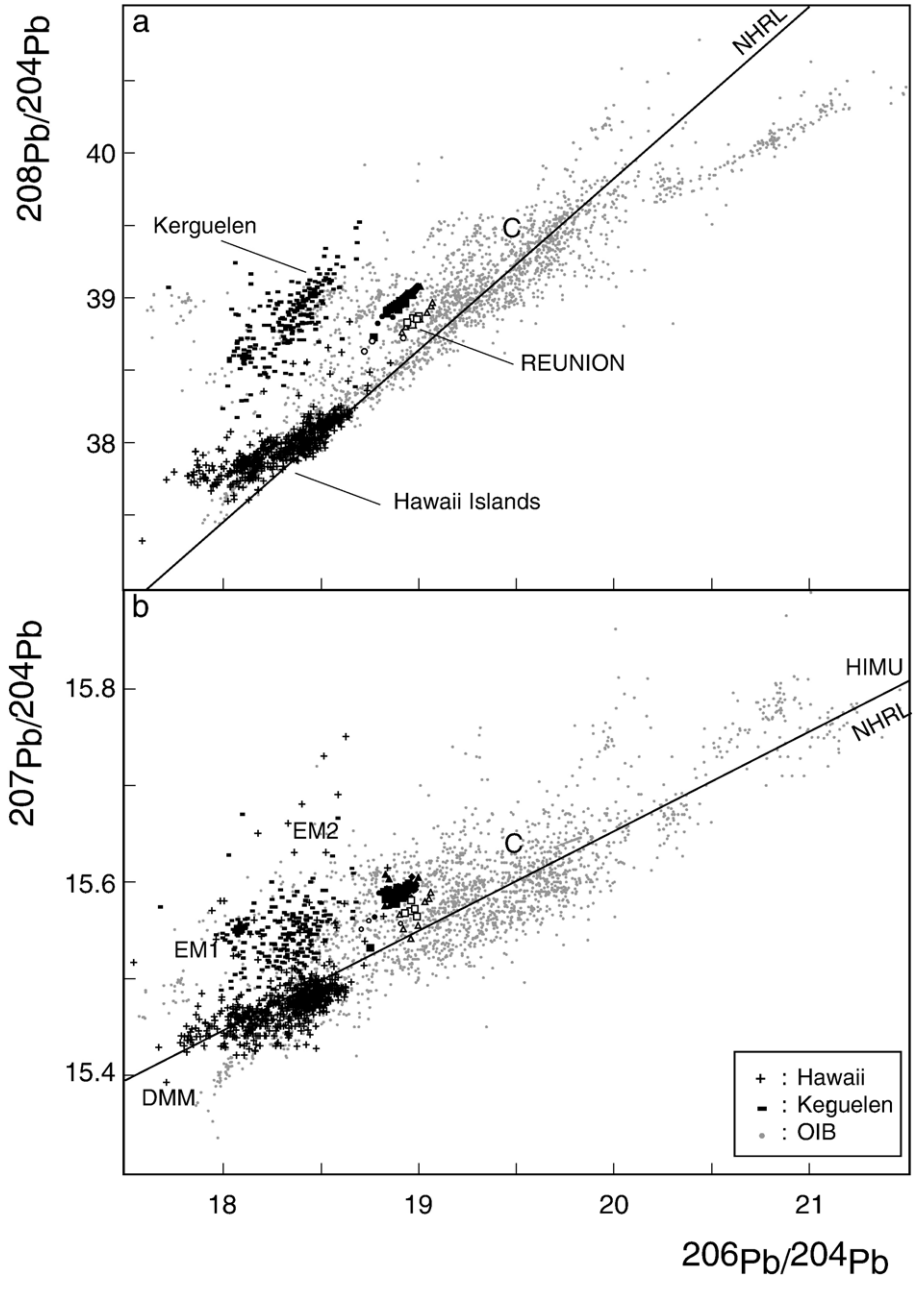

Fig. 8. (a) $^{208}Pb/^{204}Pb$ versus $^{206}Pb/^{204}Pb$ and (b) $^{207}Pb/^{204}Pb$ versus $^{206}Pb/^{204}Pb$ for Réunion lavas. The OIB, Hawaii islands and Kerguelen fields are from the GEOROC database [http://georoca.mpch-mainz.gwdg.de/georoc/]. NHRL: Northern Hemisphere Reference Line (Hart, 1984). DMM, HIMU, EM-1, EM-2 and C are from Zindler and Hart (1986), Salters and White (1998) andHanan et al. (2000). Symbols as in Fig. 4.

component analysis (PCA) carried out on the Piton de la Fournaise Pb isotope data indicates that the first principal component (a mixing line of two geochemical components) accounts for 98.2% of the total variance, while the second principal component (a third geochemical component) accounts for 1.4%, with the remaining variance essentially representing noise. Adding Sr, Nd, and Hf isotope data to the PCA increases the apparent number of components, but it has been argued that this is an artefact of the non-linear character of mixing involving the isotope compositions of different elements (Blichert-Toft et al., 2005; Debaille et al., 2006). The first and second principal components can be identified with, respectively, the C component of Hanan and Graham (1996) and a minor EM-1 component, the hallmark of the Dupal anomaly, which is interpreted as either recycled pelagic sediments (Chauvel et al., 1992) or recycled plume heads (Gasperini et al., 2000). The third component accounts for the ankaramite Trend 2′ and points towards a depleted mantle component. Adding Piton des Neiges to the PCA analysis drastically changes the situation: the first principal component now accounts for 90.8% of the total variance and the second principal component for 8.8%. The three-geochemical component representation still holds but Piton des Neiges lavas clearly have a stronger imprint of a depleted mantle component and a weaker Dupal flavor.

5.2. Small-scale geochemical variations in relation to shallow-level processes

Previous isotopic analyses of lavas from Piton de la Fournaise have revealed that compositional small-scale isotopic variations occur at very different time-scales, from thousands of years to a few tens of years, but also during the course of a single eruption (Vlastelic et al., 2005). Such small-scale compositional changes potentially may be linked to specific processes such as rate of eruption, volume of lavas, or style of the volcanic eruption.

The Rempart sequence has, on average, the most radiogenic $^{208}Pb/^{204}Pb$ and $^{207}Pb/^{204}Pb$ ratios of all the sequences studied. This series, erupted early in the formation of the old Piton de la Fournaise shield-volcano, is more than 1000 m thick (Bachélery and Mairine, 1990). The rate of volcanic eruption of this thick lava pile is difficult to evaluate given the lack of geochronological data and the numerous gaps throughout the series (Albarède et al., 1997). Nevertheless, the decrease of the $^{208}Pb/^{206}Pb$ ratio from the oldest Rempart series to 1330 m with a subsequent increase in the younger lavas is particularly striking (Supplementary data 2 in the Appendix). In principle, such a Pb isotope distribution can be explained by variation of the plume composition on a very short time-scale. However, this disagrees both with the PCA model, which suggests that 98.2% of the Piton de la Fournaise Pb isotope composition is explained by mixing between two major components, and with the steady decrease of $^{208}Pb/^{206}Pb$ observed from bottom to top of the section. Alternatively, the cause may be limited shallow-level contamination/assimilation processes either with (1) the old Paleocene oceanic crust surrounding the magma chamber or with (2) the plumbing network constituted by dykes from previous flows and cross-cut by new magmas. The top and bottom of the Rempart series are made of different types of lavas. Plagioclase-rich basalts contaminated by disaggregated gabbroic fragments have been recovered exclusively in this sequence and are located mainly at the bottom part between 700 and 900 m. These samples (RP31, RP25…) are characterized by higher $^{208}Pb/^{206}Pb$ and lower $^{206}Pb/^{204}Pb$ and $^{208}Pb/^{204}Pb$ ratios than the upper Rempart basalts and have been linked to contamination processes by the surrounding old oceanic crust (Albarède et al., 1997). Such assimilation of country rocks is typically related to periods of volcanic quiescence, for example during refilling of the magma reservoir between two eruption events (Vlastelic et al., 2005) or, more likely in the present case, to the onset of activity at a new volcanic edifice when early magmas more efficiently assimilate country-rocks. The correlation of the decrease in $^{208}Pb/^{206}Pb$ with sample location in the volcanic pile (i.e., age of the flow) identifies a temporal decrease of crustal assimilation processes (i.e., plagioclase-rich basalts and differentiated lavas with aphyric textures comprising samples below ~1000 m). Basaltic and picritic samples at the top of this series display more homogeneous Pb isotope ratios and slightly higher $^{87}Sr/^{86}Sr$, with an average of 0.70411 (samples N 900 m) versus 0.70408 (samplesb 900 m). Thus, the upper samples are interpreted as having the isotopic composition closest to that of the plume feeding Réunion volcanism. Nevertheless, it is noteworthy that throughout the Rempart lavas, erupted during approximately 237 kyr, the variation of the $^{208}Pb/^{206}Pb$ ratio is lower ($\Delta^{208}Pb/^{206}Pb = 0.0058$) than that registered by historic lavas emitted by Piton de la Fournaise between 1998 and 2002 ($\Delta^{208}Pb/^{206}Pb$ = 0.0085; (Vlastelic et al., 2005)). This highlights the generally homogeneous character of this prehistoric volcanic sequence. Moreover, the Nd and Hf isotope compositions of the Remparts basalts, excluding plagioclase-rich sample RP31, are the most homogeneous of all the studied lavas from Piton de la Fournaise. A long period of little to no activity,

approximately 70 kyr (between 290 and 219 ka), separates the Rempart from the Nez de Boeuf series (Gillot et al., 1990). The Nez de Boeuf sequence is over 200m thick and spans ~ 85 kyr (Gillot et al., 1990) with extensive discontinuities. Field observations show that the Nez de Boeuf lavas cross-cut pre-existing Rempart dykes. The Pb isotope distribution of these lavas is complex. It displays a relatively large range of Pb isotope ratios compared to the three other sequences from Piton de la Fournaise and partly overlaps compositions of both older and younger lava sequences. This feature can be related to the rapid variation of magma composition over a short time-scale but appears difficult to reconcile with the conclusions reached for the thicker and longer Rempart series. It can be consistent with a model of lava flows reacting with older solidified magmas present as a dispersed dyke system located at shallow level, though this does not explain the less radiogenic samples of the Nez de Boeuf series (i.e., samples with Pb isotope ratios out of the range of older Remparts series). Thus, the observed Pb isotope shift is more likely related to a major modification of the volcanic system between the Remparts and Nez de Boeuf eruptions, an assumption which is strengthened by the hiatus separating the two series.

The Langevin sequence, which comprises a 485 m thick sequence of lavas erupted over ~30 kyr, was erupted after a quiescent period of almost 40 kyr (Gillot et al., 1990). Compared to the Rempart sequence, it shows, on average, a clear tholeiitic affinity and significantly higher $^{208}Pb/^{206}Pb$ and lower $^{206}Pb/^{204}Pb$ and $^{208}Pb/^{204}Pb$ ratios, as well as more scattered ε_{Hf} and ε_{Nd} (Table 1). No clear decrease or increase of Pb isotope ratios versus height is evident in this sequence. In Fig. 3, all samples plot along Trend 2 except for a few samples (including the ankaramite) that define Trend 2′ together with two historic lavas. On a very short time-scale (~ 4 yr), Vlastelic et al. (2005) observed an inverse correlation between volcanic eruption rate and the $^{206}Pb/^{204}Pb$ ratio for historic lavas. On a thousand year time-scale, we observe a general decrease in the $^{206}Pb/^{204}Pb$ and $^{208}Pb/^{204}Pb$ ratios broadly positively correlated with the proportions of picritic samples erupted from Piton de la Fournaise (i.e., 1/30 for Rempart, 4/23 for Langevin and 5/21 for modern lavas). This general decrease in Pb isotope ratios is also roughly correlated with a decrease in the alkalinity index. In a hot-spot environment, most of the primary melts generated at depth tend towards a picritic composition (Farnetani and Richards, 1994; McKenzie and Bickle, 1988). In the case of the Réunion volcanoes, only a few picrites and MgO-rich samples have been found. Nevertheless, the high seismic velocities observed at depths greater than 15 km (Driad et al., 1995) could be related to the presence of abundant clinopyroxene-rich cumulates. A model including a deeper origin, rapid ascent to the surface and contamination with hydrothermal products lying on top of the oceanic basement has been proposed to explain the Pb isotope composition exhibited by picrites erupted from Piton de la Fournaise volcano in January 2002 (Vlastelic et al., 2005). In this model, Trend 2' is regarded as a mixing line between deeper cumulates, such as the ankaramite LGV14, and more "common" steady-state basalts. According to Vlastelic et al. (2005) such a "mixing process" is thought to occur preferentially during inter-eruption periods but is difficult to evaluate due to the lack of precise volume and rate eruption data for prehistoric lavas. The increase of picritic basalts suggests a possible relationship with emptying of the deep magma reservoir.

5.3. The ankaramite LGV14

Two main modes of fractionation appear to be present in Piton de la Fournaise basalts: (1) olivine (±clinopyroxene) fractionation dominates the transitional lavas of the shield stage; (2) gabbroic (olivine+clinopyroxene +plagioclase) fractionation dominates the early, mildly alkalic lavas. From the remarkable buffering of Mg and Ni concentrations, Albarède and co-authors (1997) concluded that fractionation takes place not in a magma chamber but by percolation of melts through thick piles of cumulates. Albarède et al. (1997) described ankaramite as an exception, not just because it is the only sample on the island to exhibit very large clinopyroxene phenocrysts, but also because its chemical and Sr isotope compositions make it difficult to assign this lava to any of the two fractionation trends. Its high CaO/Al_2O_3 and Sc/Yb ratios, combined with very low FeO/MgO, indicate the presence of pyroxene in the cumulus. These authors suggested that ankaramite cumulates had a deeper origin than other rock types but our new isotopic evidence presents a slightly different perspective. With respect to the rest of the Piton de la Fournaise lavas, this sample has particularly radiogenic Sr, unradiogenic $^{208}Pb/^{204}Pb$, and essentially normal Hf and Nd isotope compositions. This suggests that this particular ankaramite either formed by remelting clinopyroxene-rich cumulates hydrothermally altered by seawater or at least interacted with such rocks. An observation consistent with this interpretation is the evidence for deep hydrothermal interaction between seawater-derived fluids and plutonic materials through magmatic conduits under the southwestern flank of the

volcano (Augé et al., 1989; Lénat et al., 2000; Lerebour et al., 1989; Rançon et al., 1989). A similar model of deeper origin and rapid ascent to the surface (Albarède and Tamagnan, 1988) has been proposed to explain the Pb isotope composition of picrites erupted from Piton de la Fournaise in January 2002 (Vlastelic et al., 2005). An alternative explanation is to consider the ankaramite as a foreign 'nugget', such as a fragment of oceanic lithosphere, within the mantle plume. However, this would require that anhydrous melting of fertile or refractory lherzolite can potentially yield magmas with particularly high CaO/Al_2O_3.

5.4. Does a model of two small-scale mantle blobs explain the Réunion volcanoes?

One interesting pattern in our new data set is that the oldest lavas from Piton des Neiges (7 samples studied) have the same range of Pb isotope variations as nearly all Piton de la Fournaise lavas (80 samples). As previously mentioned, Piton des Neiges samples display significantly less radiogenic $^{207}Pb/^{204}Pb$ and $^{208}Pb/^{204}Pb$ isotope ratios at constant $^{206}Pb/^{204}Pb$ than samples from Piton de la Fournaise, with differences significantly larger than analytical errors (Table 1; Fig. 2a). Moreover, another striking feature is the greater scatter observed for Piton des Neiges samples compared to samples from Piton de la Fournaise for all isotopic systems (Fig. 3–5).

The lavas erupted during the shield-building phase of each volcano are very voluminous and bear distinct isotopic signatures (i.e., La Montagne sequence and Les Remparts series). Early shallow-level contamination/assimilation processes alone therefore cannot account for the range of isotopic differences observed between Piton de la Fournaise and Piton des Neiges lavas. Likewise, a progressive temporal change of the plume composition between Piton des Neiges and Piton de la Fournaise volcanic activity is unlikely, since both volcanoes contemporaneously erupted lavas with markedly different isotopic ratios (i.e., younger lavas from the PDN and older lavas from the PDF). The differences in isotopic composition between lavas from Piton de la Fournaise and Piton des Neiges volcanoes therefore suggest that each volcano tapped different parts of a single large heterogeneous plume comprised of two distinct small-scale blobs with different geochemical composition. The shift in location of the volcanic center between Piton des Neiges and Piton de la Fournaise activity supports the existence of two small-scale blobs. The contemporaneous eruption of lavas from both volcanoes took place during a short time span (approximately 400 kyr) and indicates that the magma production from the blob feeding Piton des Neiges waned as the next blob started to feed Piton de la Fournaise. The distance between the two volcanic edifices (around 35 km) suggests that, if magma rises vertically, each blob had a relatively small radius (≤ 10 km), which is consistent with estimates of *c.* 14 km for waves in conduits fed by a pulsating or blob-like plume (Whitehead and Helfrich, 1990). In the case of the Hawaiian plume, where the shield volcanoes are distributed into two curvilinear parallel trends with distinct geochemical characteristics, the radius of the axial part of the plume has been estimated at around 20 km (Bryce et al., 2005). The occurrence of these two distinct "trends" is interpreted in different ways. It could be related to melting of a plume concentrically zoned with a radial systematic variation of isotopic ratios (Hauri et al., 1994; Lassiter et al., 1996; DePaolo et al., 2001) or it could be ascribed to a left-right asymmetry of the plume composition (Abouchami et al., 2005). The position where the volcano trend passes over the plume (more or less closer to the plume axis) partly controls the systematic variation of the geochemical composition of the Hawaiian lavas. But a "blob" of anomalous plume material along the plume axis has to be present, in particular to take into account Mauna Loa isotopic compositions (Bryce et al., 2005). In the case of Réunion Island, the successive ascent of such small-scale blobs (as small diapirs) could explain the discrepancy between the isotopic composition of the two volcanoes as well as the distance between their centers.

In the model presented for Réunion volcanoes in Fig. 9, we assume the existence of two distinct waves from a single pulsating plume beneath the Réunion lithosphere. The oldest Piton des Neiges volcano corresponds to the impingement of the first blob. The oldest lavas from this volcano were erupted during the more alkalic phase of shield-building when the lithosphere was disrupted and the plume magmas percolated through it. In some instances, parts of this lithosphere were assimilated, which is consistent with the presence of numerous dunitic and, more rarely, wehrlitic xenoliths in Piton des Neiges primitive shield basalts (Upton and Wadsworth, 1972). Magmas erupted during disruption of the lithosphere are contaminated by shallow-level interactions, but the large volume of melt tends to reduce the influence of the contaminant end-member (Fig. 9a). In a second stage (Fig. 9b), the eruption rate is still high, but the lithosphere has been disrupted and depleted by the lavas erupted during shield growth. The isotopic characteristics of lavas emitted during this phase (intermediate series) are the most homogeneous of those erupted by Piton des Neiges. Later melting of the remaining blob material, associated

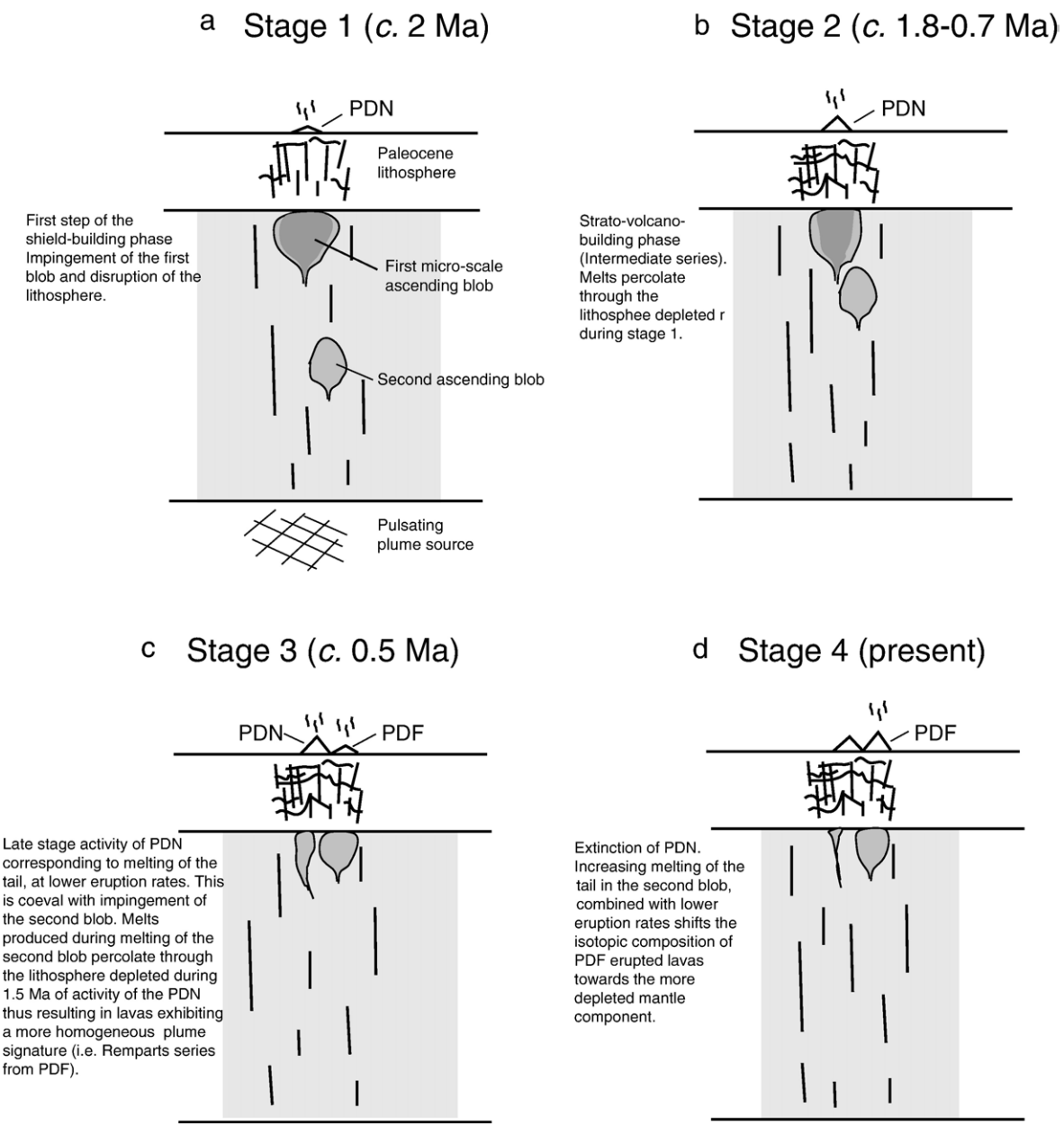

Fig. 9. Schematic model of the evolution of Piton des Neiges and Piton de la Fournaise volcanoes from Réunion Island (Indian Ocean).

with lower eruption rates, tends to shift the isotopic composition of the erupted lavas (younger series) away from the C-component composition and towards the depleted mantle component. Although lavas from the Piton de la Fournaise volcano have isotopic compositions that fit this scheme, the oldest lavas (RP), surprisingly, are the most homogeneous and the closest to the C-component composition. This can be explained by postulating that each blob is slightly different in composition (see principal component analysis) with a more important contribution from a depleted mantle component in the blob feeding the Piton des Neiges volcano. If the second blob impinged on the lithosphere very close to the first blob, this would allow the earliest magmas to percolate through an already depleted lithospheric column (Fig. 9c). This is supported by gravity anomalies suggesting a higher anomaly underlying Piton des Neiges than Piton de la Fournaise (Malengreau et al., 1999). At last, during the final stage (Fig. 9d), Piton des Neiges is extinct and Piton de la

Fournaise erupted lavas with geochemical compositions shifted towards a more depleted mantle component.

5.5. Is the Réunion plume really more homogeneous than other OIB provinces?

As discussed by Fisk et al. (1988) and Graham et al. (1990), the Réunion Island lavas show a restricted range of isotope compositions and can be considered as relatively homogeneous with respect to most other hot-spots (Figs. 6–8 and Supplementary data 3 in the Appendix). In each isotopic space, the restricted field defined by Réunion lavas is distinct and does not overlap the large domains defined by both the Kerguelen and Hawaiian hot-spots, for example. This is relevant since in both cases the plume material and the processes that affected it are distinct. Indeed, lavas from Kerguelen result from mixing between the plume-source material and several other components, in particular old continental crust (Mahoney et al., 1995; Weis et al., 1993) and lithospheric mantle modified by complex, multi-stage metasomatic processes (Mattielli et al., 1999). The geochemical characteristics of this hot-spot clearly identify temporal changes in the various mantle sources (Ingle et al., 2003). These mixing processes and interactions, as well as the longevity of this plume, account for its isotopic heterogeneity and its affinity with EM-1 and EM-2 components (Figs. 6–8 and Supplementary data 3 in the Appendix). The Hawaiian volcanoes in turn have isotopic features clearly distinct from those of the Kerguelen lavas. Previous studies have demonstrated that the Hawaiian plume material mainly consists of three distinct components – Loihi, Koolau and Kea – (Abouchami et al., 2000; Blichert-Toft and Albarède, 1999; Eiler et al., 1996; Hofmann and Jochum, 1996; Lassiter et al., 1996). In the various radiogenic isotopic spaces, Hawaiian lavas define a large domain characterized by high ε_{Hf} and ε_{Nd} coupled with low Pb isotope ratios with few samples trending towards the EM-1 end-member. As observed for the modern Réunion plume lavas, the most enriched lavas have been produced during the shield-building phase, whereas the most depleted lavas correspond to the late stage of volcanic activity. In Pb isotope space, Réunion lavas are characterized by a significantly ^{206}Pb-richer plume component compared to Kerguelen and Hawaiian lavas. The Hf and Nd isotope signatures of Réunion lavas are almost mid-way between those defining the Kerguelen field on the one hand, and the Hawaiian field on the other hand. Réunion lavas plot inside a mixing triangle of the DMM, EM-1 and HIMU components and almost perfectly in the center of the OIB field (Figs. 6–8 and Supplementary data 3 in the Appendix). The average composition of the modern Réunion plume, as defined in this study, has isotopic characteristics corresponding to the average of ocean island basalts worldwide. The modern Réunion plume presents strong isotopic similarities with the C-component, which is thought to be an end-member for MORB and plume basalt arrays and an internal component for oceanic island basalts (Hanan and Graham, 1996; Hanan et al., 2000). Compared to lavas produced by the Kerguelen and Hawaiian hot-spot activities, the modern Réunion plume generates lavas characterized by a more homogeneous and 'unmodified' plume composition. The original isotopic signal of the plume has not been significantly altered during shallow level processes.

6. Conclusion

The average Pb, Hf, Nd and Sr isotope compositions determined for the modern Réunion plume support a relatively "pure" plume mantle-source composition similar to the C-component. A small amount of depleted mantle component, closely resembling that currently measured in MORB from the Central Indian Ocean Ridge, also has been identified using principal component analysis. The imprint of this component appears to be stronger in the Piton des Neiges volcano than in the Piton de la Fournaise volcano. Through time, and independently for each of the two volcanoes, the isotopic composition of the last-stage lavas becomes more depleted than that of the shield-building stage. This coincides with a lower eruption rate and can be related either to increased shallow-level contamination processes or, more probably, to melting of heterogeneities present in the blob feeding the volcano. The isotopic features and available geophysical data from the two Réunion Island volcanoes are best explained by a two-blob model ascending through an ambient mantle and generating one volcano each. On a global scale, the modern Réunion plume appears more homogeneous than other hot-spots and, in particular, more homogeneous than the Hawaii or Kerguelen hot-spots.

Acknowledgements

We thank B. Galland for maintenance of the chemical laboratory of Géosciences Montpellier and P. Brunet (LMTG, Toulouse) for running Sr isotope analyses. We acknowledge Richard Carlson for the editorial handling and two anonymous reviewers for constructive comments. We are grateful to Ivan Vlastelic for providing unpublished Nd isotope data from historical Réunion flows and for fruitful discussions.

References

Abouchami, W., Galer, S.J.G., Hofmann, A.W., 2000. High precision lead isotope systematics of lavas from the Hawaiian Scientific Drilling Project. Chem. Geol. 169, 187−209.

Abouchami, W., Hofmann, A.W., Galer, S.J.G., Frey, F.A., Eisele, J., Feigenson, M., 2005. Lead isotopes reveal bilateral asymmetry and vertical continuity in the Hawaiian mantle plume. Nature 434, 851−856.

Albarède, F., Tamagnan, V., 1988. Modelling the recent geochemical evolution of the Piton de la Fournaise volcano, Réunion Island. J. Petrol. 29, 997−1030.

Albarède, F., Luais, B., Fitton, G., Semet, M., Kaminski, E., Upton, B. G., Bachelery, P., Cheminée, J.L., 1997. The geochemical regimes of Piton de la Fournaise volcano (Réunion) during the last 530,000 years. J. Petrol. 38, 171−201.

Albarède, F., Telouk, P., Blichert-Toft, J., Boyet, M., Agranier, A., Nelson, B.K., 2004. Precise and accurate isotopic measurements using multiple-collector ICPMS. Geochim. Cosmochim. Acta 68, 2725−2744.

Augé, T., Lerebour, P., Rançon, J.-P., 1989. The Grand Brûlé exploration drilling: new data on the deep framework of the Piton de la Fournaise volcano. Part 3: mineral chemistry of the cumulate rocks. J. Volcanol. Geotherm. Res. 36, 139−151.

Bachélery, P., Mairine, P., 1990. Evolution volcano-structurale du Piton de la Fournaise, depuis 0,53 Ma. In: Lénat, J.-F. (Ed.), Le Volcanisme de la Réunion. Clermont-Ferrand. Centre de Recherches Volcano-logiques, pp. 231−242.

Blichert-Toft, J., Chauvel, C., Albarède, F., 1997. Separation of Hf and Lu for high-precision isotope analysis of rock samples by magnetic sector multiple collector ICP-MS. Contrib. Mineral. and Petrol. 127, 248−260.

Blichert-Toft, J., Albarède, F., 1999. Hf isotopic compositions of the Hawaii Scientific Drilling Project core and the source mineralogy of Hawaiian basalts. Geophys. Res. Lett. 26, 935−938.

Blichert-Toft, I., Frey, F.A., Albarède, F., 1999. Hf isotope evidence for pelagic sediments in the source of Hawaiian basalts. Science 285, 879−882.

Blichert-Toft, J., Agranier, A., Andres, M., Kingsley, R., Schilling, J.G., Albarède, F., 2005. Geochemical segmentation of the Mid-Atlantic Ridge north of Iceland and ridge-hot spot interaction in the North Atlantic. Geochem. Geophys. Geosystems vol. 6 (Art. No. Q01E19 JAN 14 2005).

Bryce, J.G., DePaolo, D.J., Lassiter, J.C., 2005. Geochemical structure of the Hawaiian plume: Sr, Nd, and Os isotopes in the 2.8 km HSDP-2 section of Mauna Kea volcano. Geochem. Geophys. Geosystems vol. 6 (No. Q09G18 SEP 10 2005).

Burke, K., 1996. The African plate. S. Afr. J. Geol. 99, 339−408.

Campbell, I.H., Griffiths, R.W., 1990. Implications of mantle plume structure for the evolution of flood basalts. Earth Planet. Sci. Lett. 99, 79−93.

Chauvel, C., Hofmann, A.W., Vidal, P., 1992. Himu Em — the French−Polynesian Connection. Earth Planet. Sci. Lett. 110, 99−119.

Debaille, V., Blichert-Toft, J., Agranier, A., Doucelance, R., Schiano, P., Albarède, F., 2006. Geochemical component relationships in MORB from the Mid-Atlantic Ridge, 22−35 degrees N. Earth Planet. Sci. Lett. 241, 844−862.

Deniel, C., 1990. Le magmatisme du Piton des Neiges. In: Lénat, J.F. (Ed.), Monographie, pp. 115−143.

DePaolo, D.J., Bryce, J.G., Dodson, A., Shuster, D.L., Kennedy, B.M., 2001. Isotopic evolution of Mauna Loa and the Chemical Structure of the Hawaiian Plume. Geochem., Geophys., Geosystems 2, doi:10.1029/2000GC000139.

Driad, L.A., Hirn, A., Nercessian, A., Charvis, P., Laesanpura, A., Gallart, J., 1995. Crustal and upper mantle structure under the Réunion hotspot from seismic wide angle data. EOS Trans. AGU 95, F.M.S. 1995. Crustal and upper mantle structure under the Réunion hotspot from seismic wide angle data. EOS Trans. AGU 95, Fall Meeting Suppl. 587.

Duncan, R.A., Backman, J., Peterson, L., 1989. Réunion hot spot activity through Tertiary time: initial results of the Ocean Drilling Program, Leg 115. J. Volcanol. Geotherm. Res. 36, 183−198.

Eiler, J.M., Farley, K.A., Valley, J.W., Hofmann, A.W., Stolper, E.M., 1996. Oxygen isotope constraints on the sources of Hawaiian volcanism. Earth Planet. Sci. Lett. 144, 453−467.

Eisele, J., Sharma, M., Galer, S.J.G., Blichert-Toft, J., Devey, C.W., Hofmann, A.W., 2002. The role of sediment recycling in EM-1 inferred from Os, Pb, Hf, Nd, Sr isotope and trace element systematics of the Pitcairn hotspot. Earth Planet. Sci. Lett. 196, 197−212.

Farnetani, C.G., Richards, M.A., 1994. Numerical investigation of the mantle plume initiation model for flood basalt events. J. Geophys. Res. 99, 13813−13833.

Farnetani, C.G., Richards, M.A., Ghiorso, M.S., 1996. Petrological models of magma evolution and deep crustal structure beneath hotspots and flood basalt provinces. Earth Planet. Sci. Lett. 143, 81−94.

Fisk, M.R., Upton, B.G.J., Ford, C.E., White, W.M., 1988. Geochemical and experimental study of the genesis of Réunion island, Indian Ocean. J. Geophys. Res. 93, 4933−4950.

Fretzdorff, S., Haase, K.M., 2002. Geochemistry and petrology of lavas from the submarine flanks of Réunion Island (western Indian Ocean): implications for magma genesis and the mantle source. Mineral. Petrol. 75, 153−184.

Gasperini, D., Bilchert-Toft, J., Bosch, D., Del Moro, A., Macera, P., Telouk, P., Albarède, F., 2000. Evidence from Sardinian basalt geochemistry for recycling of plume heads into the Earth's mantle. Nature 408, 701−704.

Gillot, P.-Y., Nativel, P., Condomines, M., 1990. Evolution volcano-structurale du Piton de la Fournaise, depuis 0.53 Ma. In: Lénat, J.-F. (Ed.), Le Volcanisme de la Réunion. Clermont-Ferrand: Centre de Recherches Volcanologiques, pp. 243−256.

Graham, D., Lupton, J., Albarède, F., Condomines, M., 1990. A 360,000 year helium isotope record from Piton de la Fournaise, Réunion Island. Nature 347, 545−548.

Hanan, B.B., Graham, D.W., 1996. Lead and helium isotope evidences from oceanic basalts from a common deep source of mantle plume. Science 272, 991−995.

Hanan, B.B., Schilling, J.G., 1997. The dynamic evolution of the Iceland mantle plume: the lead isotope perspective. Earth Planet. Sci. Lett. 151, 43−60.

Hanan, B.D., Blichert-Toft, J., Kingsley, R., Schilling, J.G., 2000. Depleted Iceland mantle plume geochemical signature: artifact of multi-component mixing? Geochem. Geophys. Geosystems 1 (Paper number 1999GC000009).

Hanyu, T., Dunai, T.J., Davies, G.R., Kaneoka, I., Nohda, S., Uto, K., 2001. Noble gas study of the Réunion hotspot: evidence for distinct less-degassed mantle sources. Earth Planet. Sci. Lett. 193, 83–98.

Hart, S.R., 1984. The DUPAL anomaly: a large-scale isotope anomaly in the southern hemisphere mantle. Nature 309, 753–757.

Hart, S.R., 1988. Heterogeneous mantle domains: signatures, genesis and mixing chronologies. Earth Planet. Sci. Lett. 90, 273–296.

Hauri, E.H., Whitehead, J.A., Hart, S.R., 1994. The nature of entrainment in mantle plumes: a boundary layer model including the effects of temperature and stress-dependent rheologies and depth-dependent physical properties. J. Geophys. Res. 99, 24275–24300.

Hofmann, A.W., 1997. Mantle geochemistry: the message from oceanic volcanism. Nature 385, 219–229.

Hofmann, A.W., Jochum, K.P., 1996. Source characteristics derived from very incompatible trace elements in Mauna Loa and Mauna Kea basalts, Hawaii Scientific Drilling Project. J. Geophys. Res. 101, 11831–11839.

Huang, S., Frey, F.A., 2003. Trace element abundances of Mauna Kea basalt from phase 2 of the Hawaii scientific drilling project: petrogenetic implications of correlations with major element content and isotopic ratios. Geochem. Geophys. Geosystems 4 (Art. No. 8711 JUN 28 2003).

Ingle, S., Weis, D., Doucet, S., Mattielli, N., 2003. Hf isotope constraints on mantle sources and shallow-level contaminants during Kerguelen hotspot activity since ~ 120 Ma. Geochem. Geophys. Geosystems 4 Paper number 2002GC000482.

Lassiter, J., DePaolo, D.J., Tatsumoto, M., 1996. Isotopic evolution of the Mauna Loa volcano: results from the initial phase of the Hawaii scientific drilling project. J. Geophys. Res. 101, 11769–11780.

Lénat, J.F., Fitterman, D., Jackson, D., Labazuy, P., 2000. Geoelectrical structure of the central zone of Piton de la Fournaise volcano (Réunion). Bull. Volcanol. 62, 75–89.

Lerebour, P., Rançon, J.P., Augé, T., 1989. The Grand Brûlé exploration drilling: new data on the deep framework of the Piton de la Fournaise volcano. Part 2: secondary minerals. J. Volcanol. Geotherm. Res. 36, 129–137.

Luais, B., 2004. Temporal changes in Nd isotopic composition of Piton de la Fournaise magmatism (Réunion Island, Indian Ocean). Geochem. Geophys. Geosystems 5 Paper number 2002GC000502.

Luais, B., Telouk, P., Albarède, F., 1997. Precise and accurate neodymium isotopic measurements by plasma-source mass spectrometry. Geochim. Cosmochim. Acta 61, 4847–4854.

Ludden, J.N., 1978. Magmatic evolution of the basaltic shield volcanoes of the Réunion island. J. Volcanol. Geotherm. Res. 4, 171–198.

Mahoney, J.J., Jones, W.B., Frey, F.A., Salters, V.J.M., Pyle, D.G., Davies, H.L., 1995. Geochemical characteristics of lavas from broken ridge, the naturaliste plateau and southernmost Kerguelen Plateau — cretaceous plateau volcanism in the Southeast Indian-Ocean. Chem. Geol. 120, 315–345.

Malengreau, B., Lénat, J.F., Froger, J.L., 1999. Structure of Réunion Island (Indian Ocean) inferred from the interpretation of gravity anomalies. J. Volcanol. Geotherm. Res. 88, 131–146.

Mattielli, N., Weis, D., Scoates, J.S., Shimizu, N., Mennessier, J.P., Gregoire, M., Cottin, J.Y., Giret, A., 1999. Evolution of heterogeneous lithospheric mantle in a plume environment beneath the Kerguelen archipelago. J. Petrol. 40, 1721–1744.

McDougall, I., 1971. The geochronology and evolution of the young volcanic island of Réunion, Indian Ocean. Geochim. Cosmochim. Acta 35, 261–288.

McDougall, I., Compston, W., 1965. Strontium isotopic composition and potassium-rubidium ratios in some rocks from Réunion and Rodriguez, Indian Ocean. Nature 207, 252–253.

McKenzie, D., Bickle, M.J., 1988. The volume and composition of melt generated by extension of the lithosphere. J. Petrol. 29, 625–679.

Morgan, W.J., 1981. Hotspots tracks and the opening of the Atlantic and Indian oceans. In: Emiliani, C.A. (Ed.), The Sea. The oceanic lithosphere, New York, pp. 443–487.

Nativel, P., Joron, J.-L., Treuil, M., 1979. Etude pétrographique et géochimique des volcans de la Réunion. Bull. Soc. Geol. Fr. 21, 427–440.

Neal, C.R., Mahoney, J.J., Chazey III, W.J., 2002. Mantle sources and the highly variable role of continental lithosphere in basalt petrogenesis of the Kerguelen plateau and Broken Ridge LIP: Results from ODP Leg 183. J. Petrol. 43, 1177–1205.

Nohda, S., Kaneoka, I., Hanyu, T., Xu, S., Uto, K., 2005. Systematic Variation of Sr-, Nd- and PbIsotopes with Time in Lavas of Mauritius, Réunion Hotspot. J. Petrol. 46, 505–522.

Olson, J.E., 1993. Joint pattern development: effects of subcritical crack growth and mechanical crack interaction. J. Geophys. Res. 98, 12251–12265.

Oversby, V.M., 1972. Genetic relations among volcanic rocks of Réunion: chemical and lead isotopic evidences. Geochim. Cosmochim. Acta 36, 1167–1179.

Paul, D., White, W.M., Blichert-Toft, J., 2005. Geochemistry of Mauritius and the origin of rejuvenescent volcanism on oceanic island volcanoes. Geochem. Geophys. Geosystems 6, Q06007, doi:10.1029/2004GC000883.

Peng, Z.X., Mahoney, J.J., 1995. Drillhole lavas from the northwestern Deccan Traps, and the evolution of Réunion hotpsot mantle. Earth Planet. Sci. Lett. 134, 169–185.

Pin, C., Briot, D., Bassin, C., Poitrasson, F., 1994. Concomitant separation of strontium and samarium–neodymium for isotopic analysis in silicate samples, based on specific extraction chromatography. Anal. Chim. Acta 298, 209–217.

Rançon, J.-P., Lerebour, P., Augé, T., 1989. The Grand Brûlé exploration drilling: new data on the deep framework of the Piton de la Fournaise volcano. Part I: Lithostratigraphic unit and volcanostructural interpretation. J. Volcanol. Geotherm. Res. 36, 113–127.

Richard, P., Shimizu, N., Allegre, C.J., 1976. $^{143}Nd/^{146}Nd$, a natural tracer: an application to oceanic basalts. Earth Planet. Sci. Lett. 31, 269–278.

Rocher, P., 1990. Structural evolution of Piton des Neiges volcano. In: Lénat, J.F. (Ed.), Le volcanisme de la Réunion. Clermont-Ferrand, pp. 145–162.

Salters, V.J.M., White, W.M., 1998. Hf isotope constraints on mantle evolution. Chem. Geol. 145, 447–460.

Schilling, J.G., 1991. Fluxes and excess temperatures of mantle plumes inferred from their interaction with migrating ridge. Nature 352, 397–403.

Sobolev, A.V., Nikogosian, I.K., 1994. Petrology of long-lived mantle plume magmatism: Hawaii, Pacific, and Réunion island, Indian Ocean. Petrology 2, 111–114.

Staudacher, T., Sarda, P., Allegre, C.J., 1990. Noble gas systematics of Réunion island, Indian Ocean. Chem. Geol. 89, 1–17.

Todt, W., Cliff, R.A., Hanser, A., Hofmann, A.W., 1996. Evaluation of a ^{202}Pb–^{205}Pb double spike for high-precision lead isotope analysis. In: Basu, A., Hart, S. (Eds.), Earth Processes: reading the Isotopic Code. Geophysical Monograph. American Geophysical Union, vol 95, pp. 429–437.

Upton, B.G., Wadsworth, W.J., 1972. Peridotitic and gabbroic rocks associated with the shield-forming lavas of Réunion. Contrib. Mineral. Petrol. 35, 139−158.

Vlastelic, I., Staudacher, T., Semet, M., 2005. Rapid change of lava composition from 1998 to 2002 at Piton de la Fournaise (Réunion) inferred from Pb isotopes and trace elements: evidence for variable crustal contamination. J. Petrol. 46, 79−107.

Weis, D., Frey, F.A., Leyrit, H., Gautier, I., 1993. Kerguelen archipelago revisited — geochemical and isotopic study of the Southeast Province Lavas. Earth Planet. Sci. Lett. 118, 101−119.

White, W.M., Cheatham, M., Duncan, R., 1990. Isotope geochemistry of Leg 115 basalts and inferences on the history of the Réunion mantle plume. Proc. Ocean. Drill. Prog. Sci. Results 101, 53−61.

White, W.M., Albarède, F., Telouk, P., 2000. High-precision analysis of Pb isotope ratios by multi-collector ICP-MS. Chemical Geology 167, 257−270.

Whitehead, J.A., Helfrich, K.R., 1990. Magmas waves and diapiric dynamics. In: Ryan, M.P. (Ed.), Magmas transport and storage. John Wiley, New York, pp. 53−76.

Xu, J.F., Castillo, P., 2004. Geochemical and Nd−Pb isotopic characteristics of the Tethyan asthenosphere: implications for the origin of the Indian ocean mantle domain. Tectonophysics 393, 9−27.

Zhang, S.Q., Mahoney, J.J., Mo, X.X., Ghazi, A.M., Milani, L., Crawford, A.J., Guo, T.Y., Zhao, Z.D., 2005. Evidence for a widespread Tethyan upper mantle with Indian ocean-type isotopic characteristics. J. Petrol. 46, 829−858.

Zindler, A., Hart, S.R., 1986. Chemical geodynamics. Annu. Rev. Earth Sci. 14, 493−571.